Heliyon 9 (2023) e12846

Contents lists available at ScienceDirect

Heliyon

journal homepage: www.cell.com/heliyon

Research article

Automated identification and assessment of environmental noise sources

Jure Murovec *, Luka Čurović, Anže Železnik, Jurij Prezelj

Faculty of Mechanical Engineering, University of Ljubljana, Aškerčeva cesta 6, 1000, Ljubljana, Slovenia

ARTICLE INFO

Keywords:
Immission directivity
Spatial filtering
Noise source classification
Environmental noise
Microphone array
Automatization of measurements

ABSTRACT

Noise pollution is one of the major health risks in urban life. The approach to measurement and identification of noise sources needs to be improved and enhanced to reduce high costs. Long measurement times and the need for expensive equipment and trained personnel must be automated. Simplifying the identification of main noise sources and excluding residual and background noise allows more effective measures. By spatially filtering the acoustic scene and combining unsupervised learning with psychoacoustic features, this paper presents a prototype system capable of automated calculation of the contribution of individual noise sources to the total noise level. Pilot measurements were performed at three different locations in the city of Ljubljana, Slovenia. Equivalent sound pressure levels obtained with the device were compared to the results obtained by manually marking individual parts of each of the three measurements. The proposed approach correctly identified the main noise sources in the vicinity of the measurement points.

1. Introduction

Noise is defined as any sound we hear that is annoying. Unlike other environmental factors (e.g., electromagnetic fields, air pollutants), humans can perceive noise through their own (auditory) system, which is constantly stimulated by events in the acoustic environment.

Noise causes agitation, irritability, disturbs sleep, affects psychophysical state, reduces performance, concentration, and learning ability, and can trigger changes in social behaviour, [1–4]. Prolonged exposure to noise can lead to cardiovascular disease, [5–9], and metabolic disorders, which can develop into a disease state such as type 2 diabetes, [10–14]. Noise agitation causes atrial fibrillation, [15,16], and contributes to the worsening of asthma symptoms in adults [17,18]. As a result, psychoactive medications are increasingly used due to excessive noise, [19–21]. Prolonged exposure to noise and agitation due to noise, especially road noise, also increases the likelihood of obesity, [22], and a negative impact on cognitive abilities has been demonstrated, [23,24].

In Europe, adverse public health effects of noise also have negative economic impacts. The cost of noise pollution is estimated at 35 billion euros for anxiety, sleep disturbance at 34 billion euros, ischemic heart disease at 12 billion euros, and cognitive impairment in children at 5 million euros. Monetary costs may also result from lower property prices, lost work days, and restricted land use opportunities, [25].

The time, amplitude, frequency, and location-dependent complexity of environmental noise, as well as the simultaneous operation

* Corresponding author.
E-mail address: jure.murovec@fs.uni-lj.si (J. Murovec).

https://doi.org/10.1016/j.heliyon.2023.e12846
Received 26 September 2022; Received in revised form 3 January 2023; Accepted 4 January 2023
Available online 9 January 2023

of various sources, make it difficult to determine and deal with the negative effects of noise pollution. Many studies have shown that traffic is one of the major sources of noise pollution, especially in urban areas, particularly in the form of road traffic, rail traffic, airports and port activities [26–32]. Furthermore, mechanized industry is one of the largest contributors to noise, affecting a large portion of the working population. Tonal and harmonic noises predominate in rotating and reciprocating machinery, and a wide range in fluid power systems. Residential areas are also affected by noise from nearby businesses, construction sites, and rooftop installed systems (heat pumps, air conditioners). Exposure to environmental noise is a time-dependent process. Many noise sources don't operate periodically, resulting in sound pressure level variations on various time scales, from 1 s (impulse sound) on the one hand to meteorological seasons on the other, which are influenced by weather and human activities, [33,34]. In addition to the time domain, noise sources are also diverse in the frequency domain. Due to the different mechanisms of sound generation, road traffic is a typical example of a broadband noise source. Tonal and high-frequency noise is generated by various warning sirens, while specific examples include high-speed trains and jet overflights. In general, environmental noise is defined in many studies and books with a frequency range from 20 Hz to 10,000 Hz, [35–40].

2. Background

A common task in conducting environmental noise measurements is to identify and evaluate each noise source and its contribution to the total noise level. Reducing noise pollution has been shown to be most effective at the source itself. Identifying the noise source in question becomes difficult if the sound pressure level it generates is lower than that of the other noise sources in the vicinity of the measurement point (Fig. 1).

The operation and generation of noise is random most of the time. This requires the presence of personnel during measurements. Working conditions must be documented and random sound events must be excluded. Common measurement techniques include: a) listening to the entire recording in the laboratory, b) excluding the selected noise source, which allows indirect comparison and calculation of its contribution to the total level, and c) improving the signal-to-noise ratio (SNR) by getting closer to the selected noise source, [41,42].

Sometimes none of the three techniques can be used. Noise sources often cannot be shut down (large industrial plants, ports, train stations, refineries, airports, construction sites, etc.) and coincident operation of multiple sources has significant effects on the total noise level. In addition, more often than not, we unable to get to the noise sources as close as we would desire. Control measurements are required when modelling sound propagation. Only both approaches together provide a good assessment for evaluating multiple noise sources and their significance. Operating times, geometry, terrain topography, etc. must be carefully defined. Working with different software and different propagation models increases the uncertainty of the calculations, and the constant updating of standards and laws only deepens the problem. Therefore, the variability of the results is hidden at the administrative level, [29,43,44]. Several measurements must be made at different locations to extrapolate the values to a larger area using noise modelling, [43,45–52]. Continuous noise measurements are and always will be an important source of information. Unfortunately, the current approach is expensive due to long measurement times and sophisticated equipment. Only trained and experienced personnel can produce credible results. To reduce the cost of identification of noise sources, we need to automate environmental noise measurements. Exclusion of residual noise sources and background noise must become more efficient. We humans have evolved to the point where we can perceive and assess the acoustic scene quite easily. But the development of algorithms has allowed computers to better extract information to automate a variety of human tasks. An environmental noise classification system that mimics the actions of the human expert is the next logical step in reducing the cost of measurements. If we can automate the evaluation of different noise sources and their contribution to the total noise level, the fight against noise pollution can be greatly improved. People use sound pressure level (SPL)

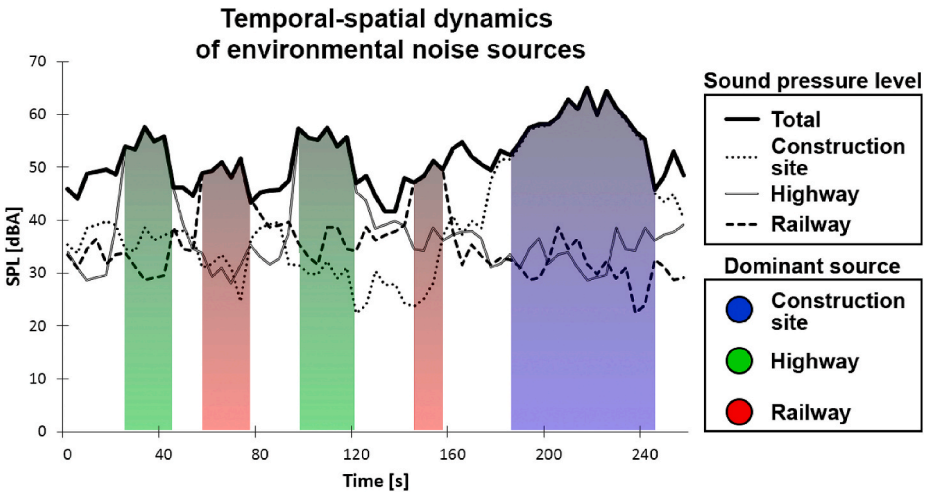

Fig. 1. Sound pressure levels from multiple sources. Measurements with a single microphone can only record the combined sound pressure level.

threshold, the direction of the noise source, and their knowledge and experience of different sounds to classify noise events in our environment. In the next sections, we describe our proposal to replicate the manual measurement process by using a microphone array for spatial filtering and unsupervised learning to identify different noise sources.

3. Methods

3.1. Source localization

In recent years, the acoustic camera has become an indispensable device for localization and visualization of noise sources. Its popularity in various industries and acoustic research has spawned several variants of arrays for the detection of sound emission. Many versions are large and have a large number of sensors, which makes them unsuitable for continuous measurements, [53–59], especially in the low frequency range, [60–68]. Microphone arrays for environmental noise measurements are more or less limited to single use cases and for the purpose of increasing SNR by forming a synthesized signal from all microphones, [53–55,69–77]. Environmental noise measurements assume far-field conditions and sound wave propagation can be simplified because the low-frequency wavelengths are many times smaller than the distances between different noise sources and the measurement point. A two-dimensional and ground-parallel sound propagation is assumed and only the azimuthal direction of the sound events is enough for a sufficient detection of the arrival direction (DAO) (Fig. 3.a). A small horizontal 4-channel array with a diameter of 30 mm was developed and coupled to an analogue-to-digital converter with a 192 kHz sampling rate (Fig. 2.a). Pairing the device with a class 1 sound level meter (SLM), as shown in Fig. 2.b, provided us with calibrated sound pressure level values.

The simultaneous acquisition of four sound signals is processed for the purpose of localizing the sound source on a two-dimensional plane. The simplicity of the delay-and-sum algorithm (DAS) and average square difference function (ASDF) enabled to combine all six pairs of microphones. The method of delay, subtract and sum (DSS) was developed by implementing the concepts of differential microphone arrays. By synergizing two different approaches, the algorithm allows the system to be computationally inexpensive while still detect the direction of sound emission in the frequency range of most of environmental noise sources. The combination of array size and algorithm performance have been tested in our previous studies, [42,78–81]. ASDF is applied to all individual microphone pairs, which are then summed up. The essence of the DSS algorithm is shown in Fig. 3. The individual microphone pairs provide a 180° mirrored ASDF (Fig. 3.b), but when we combine their results, we obtain a rather narrow beam in the direction of the most dominant source (Fig. 3.c).

The known equivalent sound pressure level $L_{A,eq,T}$ is extended into the spatial domain by including the detection of DOA within the "fast" time constant t of 125 ms. It is applied as the sum of all noise sources from 0 to 2π near the measurement point in the time interval T. The most dominant direction (φ) of the noise immission is calculated and stored together with the value of the instantaneous SPL L_p in time t. The immission directivity describes the temporal-spatial dynamics of environmental noise, [42,78–81]. The inclusion of the spatial domain helps to reveal the details of the acoustic scene and allows the implementation of new features to better identify and classify the dominant noise sources. Eq. (1) defines the immission directivity:

$$L_{A,eq,T} = 10 \log\left[\frac{1}{T}\int_0^T \int_0^{2\pi} 10^{\frac{L_p(t,\varphi)}{10}} d\varphi dt\right] \tag{1}$$

The equivalent level $L_{A,eq}$ is not able to differentiate between scenarios where multiple sources are present near the measurement point. Therefore, the parameters currently used in environmental noise measurements are in some sense insufficient for the study of the acoustic scene. The immission directivity establishes a link between the location of sources and their contribution to the total noise

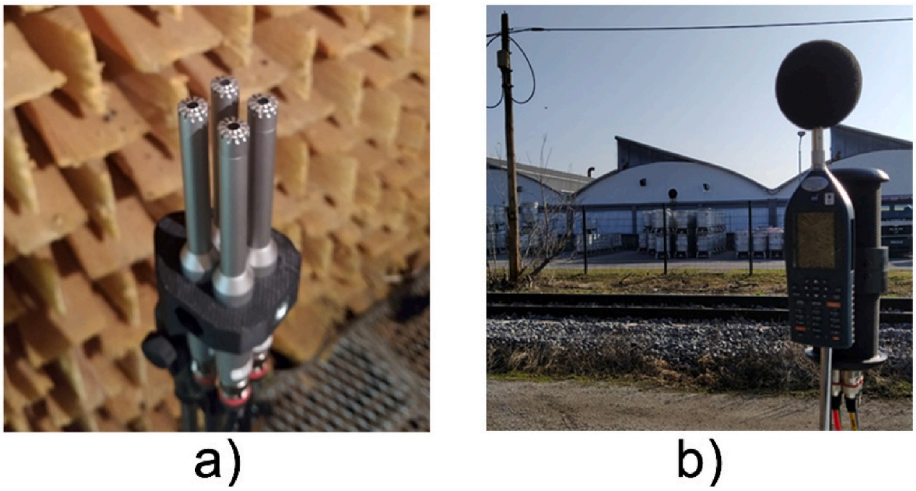

Fig. 2. a) Microphone array in anechoic chamber, b) Prototype paired with calibrated SLM for noise measurements.

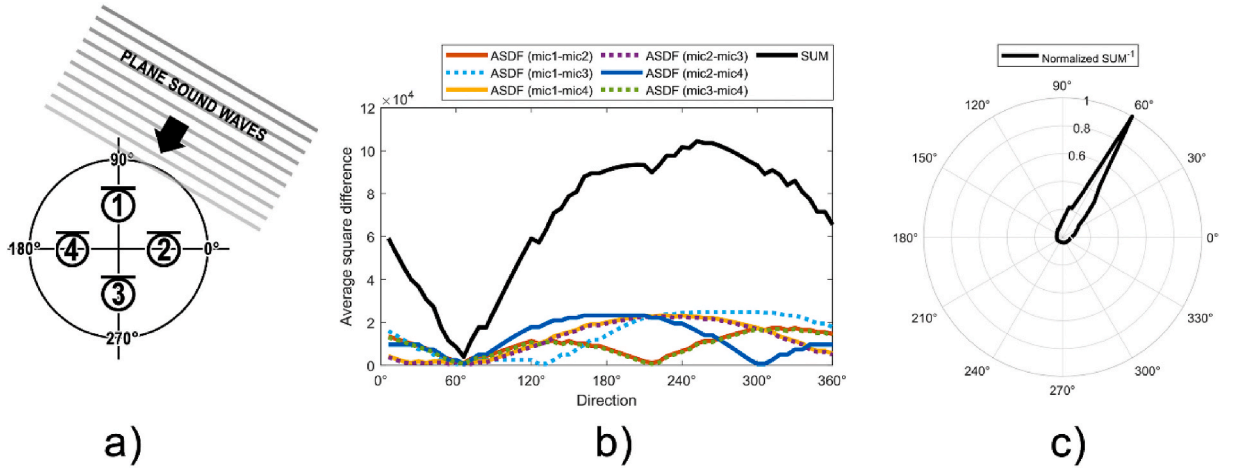

Fig. 3. DOA detection with DSS algorithm: a) Plane sound waves are detected by a microphone array, b) ASDF is calculated for each pair of microphones, c) Beam pattern of the detected noise source is generated.

level. With its introduction, the lengthy, costly, and detailed measurements are no longer necessary. The concept of immission directivity does not require any post-processing. Three environmental noise scenarios with three different noise sources were simulated. Their contribution to the total sound pressure level can be seen in Fig. 4. Although all three examples have the same $L_{A,eq}$ of 64 dBA, the immission directivity polar plot reveals their differences.

If we look at the lobes of the immission directivity from Fig. 4.a, we can see that the noise sources are relatively large and their individual contribution to $L_{A,eq}$ is comparable. On the other hand, the contribution of noise source 3 in the example in Fig. 4.b is very large. The narrow lobe indicates that the source is either very distant or very small with respect to the measurement point. With an operating probability of $P = 0{,}85$, the almost continuous operation outweighs the contributions of noise sources 1 and 2. The third example is shown in Fig. 4.c, where two noise sources operate with similar probability but different L_p at the immission point (mean value of 65 dBA for noise source 1 and 70 dBA for noise source 2). All parameters of the simulation are written in Table 1.

The traceability of SPL to the units of SI is possible, since the immission directivity values are determined with a class 1 SLM. The coupling of the presented system with a calibrated instrument means that the results can be used as legally valid.

The concept of immission directivity can be applied to another new feature: Source dominance Θ. With exclusion of $L_{A,eq}$, the microphone array computes values from all observed directions within each integration time of 125 ms. Viewing all values simultaneously in the polar diagram of the immission directivity indicates how dominant the main noise source is compared to other noise sources or/and the acoustic scene as a whole. The polar diagram approaches a circular shape when all observed directions have similar values, which means that there is no obvious noise source around the measurement point. As the dominance of the noise source increases, the beam becomes narrower and the shape of the polar plot diagram becomes more asymmetric. The source dominance Θ is calculated with Eq. (2):

$$\Theta = 1 - \frac{\sum_{i=1}^{D} \sum ASDF_i^{-1}}{D \sum ASDF_{max}^{-1}} \tag{2}$$

The range of source dominance Θ is between 0 and 1. The maximum value within the observed directions is $\sum ASDF_{max}^{-1}$, and is used to normalize the feature Θ. The presence of a dominant noise source causes the value to approach 1, as does the sum in the right part of Eq. (2). In contrast, if there is no distinct noise source and only background noise is present, the sum of the $\sum ASDF^{-1}$ values for all directions is equal to the number of observed directions D and the value of Θ approaches 0 in this case. Exclusion of measurement sections without a dominant noise source is possible by spatial filtering. This significantly reduces irrelevant data and speeds up computation, identification and classification of noise sources. The calculation of their contribution to the total noise level can be automated. Signals from multiple microphones can be used to synthesize a signal for improved SNR, further enhancing feature extraction and thus classification of individual noise sources. Three different examples of noise source dominance Θ are shown in Fig. 5. The detected direction of dominant noise source and L_p plotted against time can be seen in Fig. 5.a. The beam pattern in example A is narrow and shows a very dominant source. When the beam pattern approaches a circular shape, there is no distinct noise source, bringing the value of Θ for example B close to 0. Compared to example A, example C shows a slightly less dominant noise source located in a different direction. In Fig. 5.b we can see the comparison of Θ values for all three examples that demonstrate how the introduction of spatial domain can be used to automate and improve the process of environmental noise measurement.

3.2. Source classification

So far, more or less all classification algorithms have been developed in combination with many different types of signal features. In

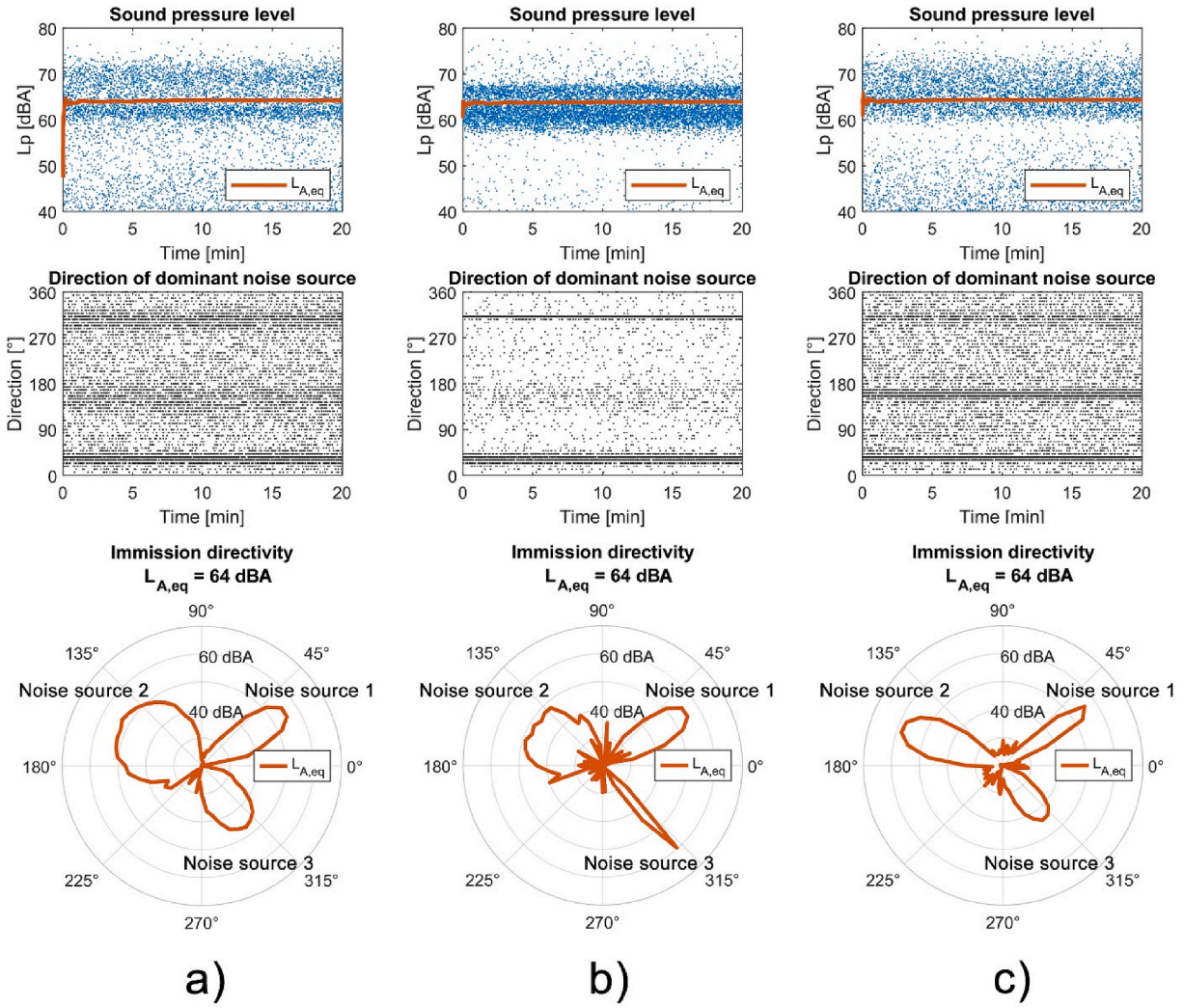

Fig. 4. Three different scenarios with three different noise sources with different parameters and contributions to the total noise level at the immission point.

Table 1
Immission directivity simulation parameters.

		Noise source 1	Noise source 2	Noise source 3
a)	L_p	65 dBA ± 5 dBA	70 dBA ± 2 dBA	62 dBA ± 1 dBA
	Probability of occurrence P	0,3	0,15	0,2
	Direction of arrival	36° ± 6°	162° ± 18°	312° ± 12°
b)	L_p	65 dBA ± 5 dBA	70 dBA ± 4 dBA	62 dBA ± 2 dBA
	Probability of occurrence P	0,25	0,05	0,85
	Direction of arrival	36° ± 6°	162° ± 18°	312° ± 1°
c)	L_p	65 dBA ± 2 dBA	70 dBA ± 3 dBA	62 dBA ± 1 dBA
	Probability of occurrence P	0,25	0,2	0,1
	Direction of arrival	36° ± 3°	162° ± 6°	312° ± 9°

the early days of research, the goal was to develop a universal method for classifying all possible noise sources. However, this proved impossible, and ad hoc solutions were developed for specific types of environmental noise sources. Artificial neural networks (ANNs) have proven to outperform other classification algorithms in general, [82–89], but the learning process of the model requires a large amount of data if we want to fine-tune the classifier, [28,90,91], which is eventually developed mostly for a specific type of noise source, [92]. ANNs can be divided into two different groups: unsupervised and supervised. A variant of the unsupervised and competitive feed-forward types are self-organising maps (SOMs). They do not require training data for the learning process, as they

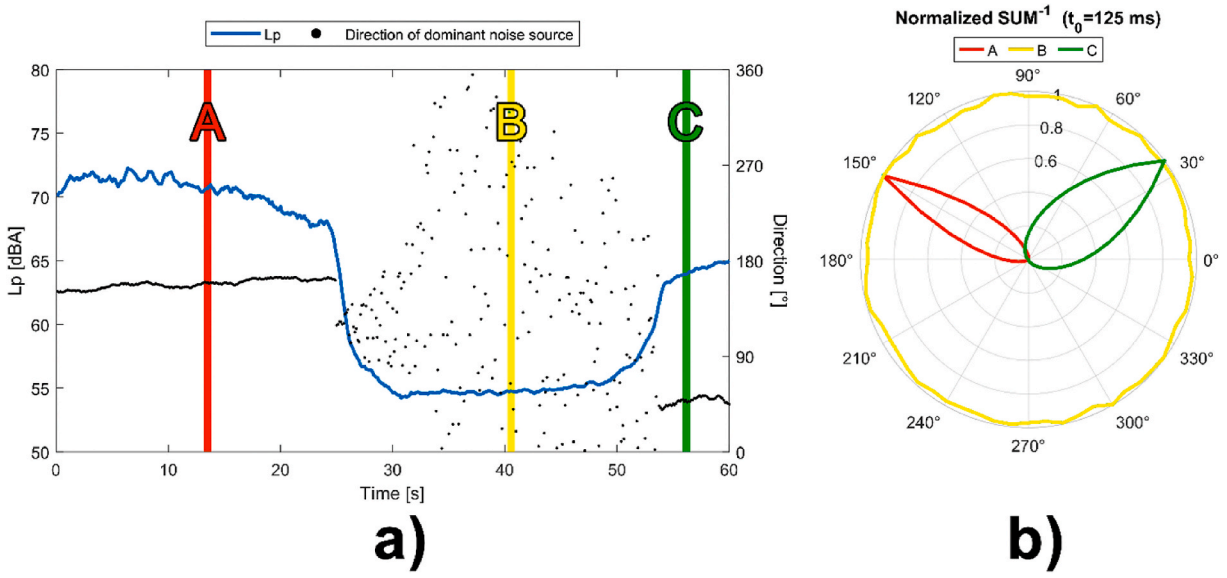

Fig. 5. a) Sound pressure level and the detected direction of the dominant noise source plotted against time, b) Three different examples of source dominance Θ behaviour.

discover and thrive on presented data's statistical similarities. The input space is then automatically clustered into different classes. A SOM consists of nodes or neurons and can be visualized as a grid-like neural network array. The radius of the neighborhood is determined by the number of neurons in the neighborhood of the best matching unit (BMU)/winning neuron. Each node is connected to weight vectors of the same dimension as the input space and at a specific position in the output space (map). Self-organising Kohonen neural networks have two layers, an input layer and an output layer, called the competitive layer. Each input neuron is connected to each neuron in the output layer, the latter being organized as a two-dimensional grid, [93].

The growing self-organising network (GSOM) uses automatic addition and subtraction of neurons and thus represents a more complex model of the fixed structure of the classical SOM. Thomas Villmann and Hans-Ulrich Bauer defined the GSOM in 1997, [94], and highlighted its main advantages in classifying the unknown structure of the input data. The topology of the output space is not fixed and is adjusted, similar to the neuron weights of the input space.

Unsupervised learning has been shown to be comparable to other methods, citing real-time use as an advantage, since no preliminary data needs to be introduced to the classifier, [95,96]. SOM has been used in a number of studies for fault diagnosis, [97–101], and has been shown to be a useful classification tool for vibration and acoustic signals. Based on a literature review of sound classification, unsupervised learning is not that commonly used because most recognition operations involve the classification of specific sounds. However, when working with larger datasets, unsupervised learning has been used to identify noise sources in water, [102, 103], predict traffic noise, [104–106], and some research has been conducted on the general classification of noise sources in urban environments, [107–112]. In classification algorithms are only one half of an accurate classification system. The selection of appropriate features is equally, if not more, important. The science of human sound perception is called psychoacoustics and it studies the connection between the physical variables (physics) of sound and our sensory perception (psychology), [113]. Research on the use of psychoacoustics in the classification of environmental noise sources is very limited, [114–117], although its applicability and importance in this field has been demonstrated in recent years by many studies, [118–124], and its implementation in the standard ISO/TS 12913-2: 2018.

The derivative and log dt/dp of the recorded sound included in this study provided an extended set of features. Newton's difference quotient was used as a simple differentiation method, while the nonlinear transformation of the recorded signal in terms of log dt/dp was used as a decompressor. In this way, attenuation of large signal changes and amplification of smaller changes are achieved. Both techniques were presented and tested in one of our previous studies, [125]. Crest factor and zero crossings were added to the psychoacoustic features of loudness, sharpness, roughness, tonality, and fluctuation strength. These seven features were extracted from each input signal (original signal, its derivative, and log dt/dp) and formed a final vector with 21 values that represented the GSOM input space.

3.3. Automation of measurements

In recent years, we have done a lot of research on microphone arrays and environmental noise measurement. We have tried to mimic the human ability of acoustic spatial filtering as much as possible, [42,78–81,126,127]. The use of spatial domain offers great potential for better identification of individual noise sources and to better understand their temporal and spatial dynamics. State-of-the-art approach to the identification, evaluation, and classification of environmental noise sources is presented in this paper.

To mimic the human ability to spatially filter the acoustic environment (i.e., the Cocktail-Party effect), we have done much research and development in recent years in the area of microphone arrays for measuring environmental noise, [42,78–81,126,127]. The implementation of the spatial domain to environmental noise measurements offers exceptional potential for more efficient identification of individual sources and clearer representation of the temporal and spatial dynamics of environmental noise. In this paper, we present a state-of-the-art approach for identifying environmental noise sources.

The microphone array represents the use of our two ears, and simultaneous listening to all directions around the measurement point allows the calculation of the immission directivity and source dominance Θ. Reduction of data needed for correct noise source classification is possible through spatial filtering, while the synthesized signal from four microphones improves SNR, making noise source detection even more accurate. GSOM enables wide applicability of the device because noise sources vary in the environment, as each acoustic scene is different from another. Psychoacoustic features that directly describe human perception of sounds are perfect for an application where we want to mimic the actions of experts. The set of features is expanded by manipulating the acquired sound signal in the form of its derivative and log dt/dp, so that the input vector for the GSOM consists of 21 single-valued features. The reduced dimensionality of the input data enables real-time operation and speeds up the classification and identification environmental noise sources.

The introduced elements of the device allow faster, more reliable, more objective and less expensive measurements. This is a step towards improving our health and the environment in which we live. Unsupervised learning, the use of spatial domain, psychoacoustic and other features allowed the development of an instrument that can determine the contribution of each noise source to the total noise level. By modernising the measurement process, indirect reduction of noise exposure is possible, resulting in less harmful effects on human well-being and health. The presented approach represents a paradigm shift in noise measurement and control. The proposed system was evaluated with three in situ measurements in the Slovenian capital Ljubljana.

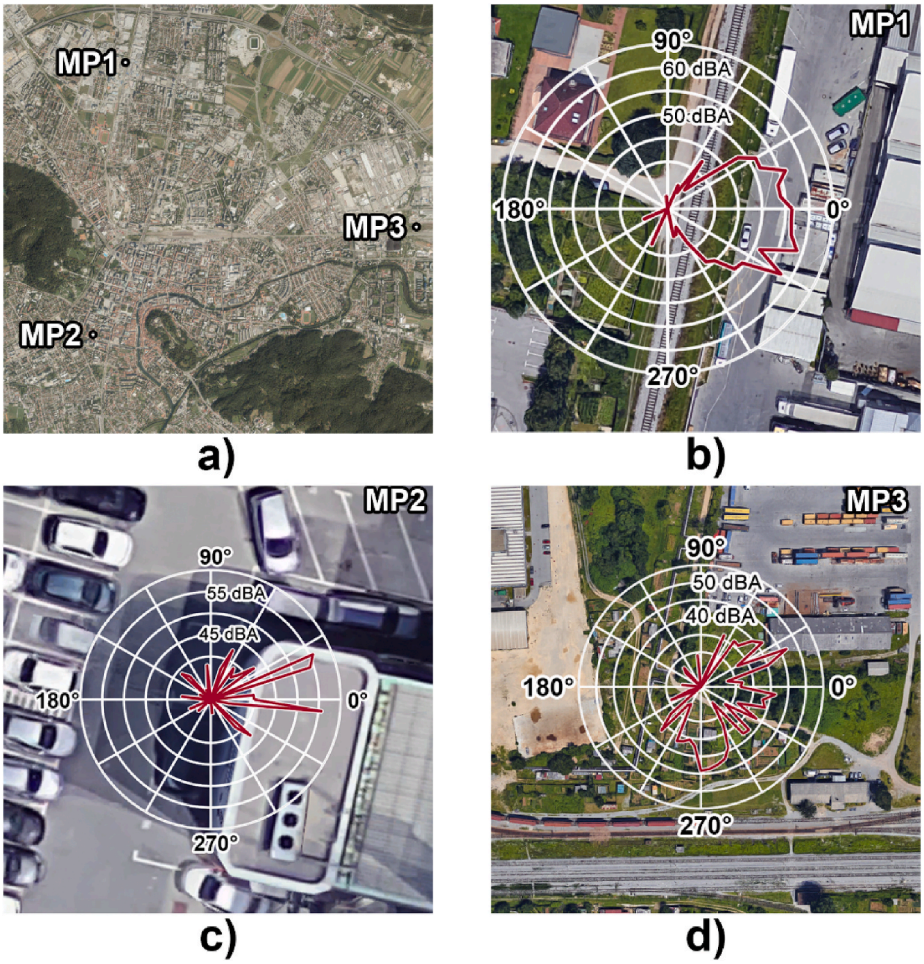

Fig. 6. a) Location of the measurement points in Ljubljana, b) Immission directivity for the measurement point near the railroad and the warehouse (MP1), c) Immission directivity at the parking lot of the Faculty of Mechanical Engineering (MP2), d) Immission directivity in the train station Moste (MP3), [128].

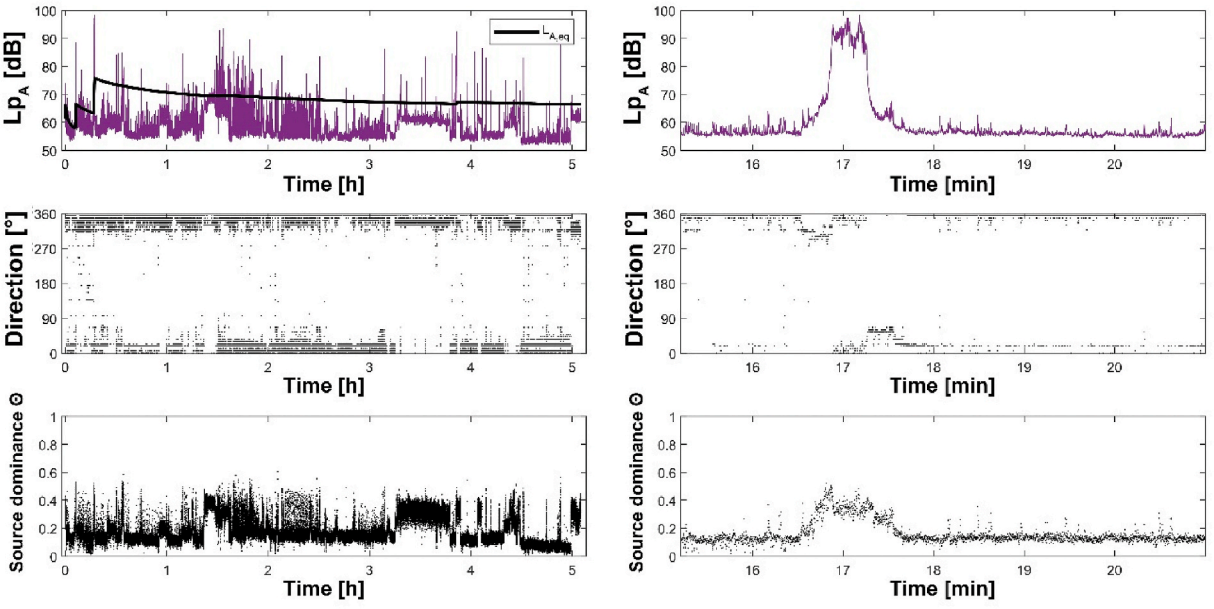

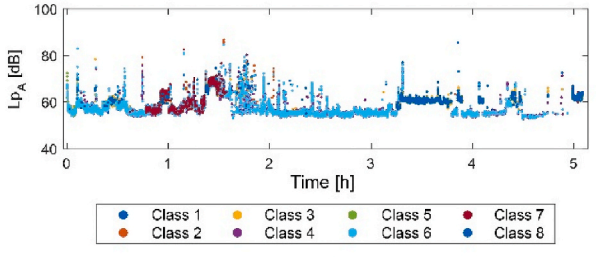

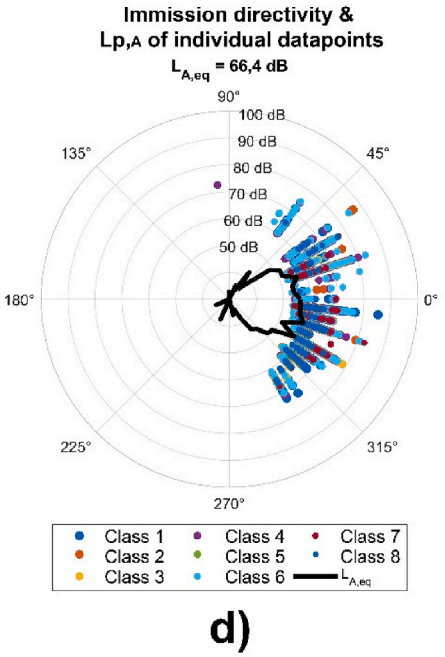

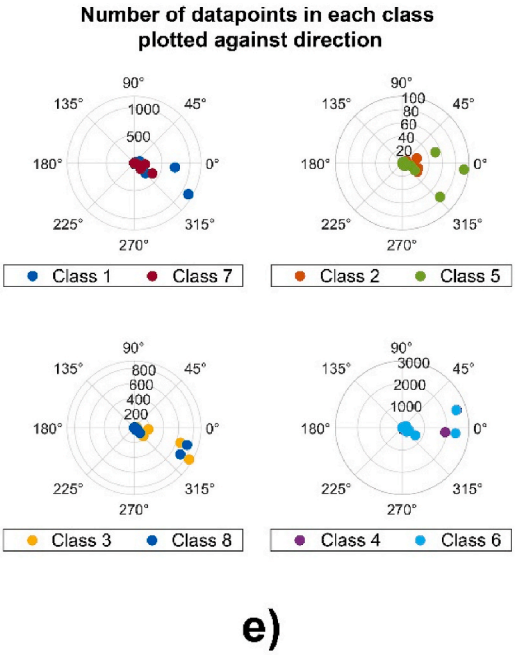

(caption on next page)

Fig. 7. Recorded data of $L_{p,A}$, direction and source dominance Θ from MP1 of: a) The entire measurement, b) Train pass-by. Classified data points from MP1 plotted against: c) Time and $L_{p,A}$, d) Direction and $L_{p,A}$ (together with immission directivity), d) direction by their total number in each class.

4. Experimental results

To properly test our system, described in chapter 3.1, three separate experiments were conducted in three different environments. Measurements were taken near different noise sources to represent the typical environmental noise assessment. The equivalent sound pressure levels of the noise sources were automatically determined by the apparatus and then compared to those of post-processing by a human expert. For each individual measurement, 5 h of data were collected, and classification took between 2 and 3 min to determine the number of classes (i.e., noise sources). The spatial resolution of the DOA detection was 6°, resulting in 60 observed directions by the microphone array on a plane parallel to the ground. The presented system was coupled with a SLM Norsonic 140, which provided calibrated results of the sound pressure level. The three measurement points were located in the vicinity of the Slovenian capital Ljubljana (Fig. 6.a), and the experiments were conducted between 9 a.m. and 6 p.m.

The measurement points (MP) seen in Fig. 6 were:

- MP 1: Industrial zone Šiška (46°04′44″ N, 14°30′13″ E),
- MP 2: Parking lot – Faculty of Mechanical Engineering (46°02′49″ N, 14°29′54″ E),
- MP 3: Vicinity of the train station Moste (46°03′35″ N, 14°32′58″ E).

4.1. Industrial zone Šiška

The first measurement (MP1) took place in the immediate vicinity of the railroad and warehouses in the Šiška industrial zone (IZ). In addition to trains and ventilation systems, noise was occasionally caused by unloading trucks and forklifts. The location of the measurement point and the calculated immission directivity is shown in Fig. 6.b.

Immission directivity shows that practically all the noise came from the east in the direction of the railroad, the production and loading areas, and the warehouse of the industrial complex. The immission was more or less evenly distributed with slightly higher values at 330° and 342°. Fig. 7.a shows the overall movement of the sound pressure level, the dominant direction and the source dominance as a function of time. All three parameters show the dynamics of the noise within the 5-h measurement. Short-term high sound level values were caused by passing trains. The increase in source dominance and the change in dominant direction are consistent with the change in $L_{p,A}$. Fig. 7.b shows a more detailed change of the recorded parameters. It can be clearly seen that a train came from the south side (at 270°) and continued toward the north (0°). The source dominance Θ reached a value above 0.4 when the train was closest to the measurement point. The stability of the determined dominant direction was affected because the apparatus was placed too close to the tracks.

The individual sound events were then classified to determine the contribution or equivalent level value of each noise source in the vicinity of the measurement site. As a threshold for spatial filtering, we chose a value of 0.1 for the source dominance characteristic and an angle of 9° for the stationarity of the incident sound direction. These two boundaries were chosen based on the data in Fig. 7.a. The occurrence of individual classified groups is shown in Fig. 7.c. The eight identified classes roughly show the four different sections. Class 4 and 6 sound events were present during most of the measurement and included lower sound level values. The other two prominent sections of the measurement are classes 3 and 8 in the fourth hour of the measurement and 1 and 7 at the end of the first and beginning of the second hour of the measurement.

The polar plot on Fig. 7.d shows the sound pressure level of individual classified data points in relation to their direction along with the immission directivity. Due to the spatial and temporal dynamics of noise at MP1, the large number of data points is also represented by their total number in each class, as can be seen in Fig. 7.e. We found that a large part of the data points were excluded from the classification and consequently from the calculation of the noise metrics due to nonstationarity of the sources because of their proximity (train) and the size of the source itself (industrial warehouse).

Classes 4 and 6 contain the most datapoints and are directed towards the ventilation on the walls of the warehouses. Classes 2 and 5 contained the fewest points, which were relatively scattered in the range from 315° to 45°, indicating the noise of passing trains. The remaining four classes more or less pointed towards the southeastern part of the production areas, where the loading/unloading of trucks took place.

Table 2
Calculated values of $L_{A,eq}$ for each class from spatially filtered data recorded at MP1.

Source	$L_{A,eq}$	Source	$L_{A,eq}$
Class 1	65,8 dBA	Class 7	66,4 dBA
Class 2	73,6 dBA	Class 5	60,3 dBA
Class 3	63,2 dBA	Class 8	61,8 dBA
Class 4	58,8 dBA	Class 6	61,4 dBA
All classes collectively	**62,6 dBA**	**Entire measurement**	**66,4 dBA**

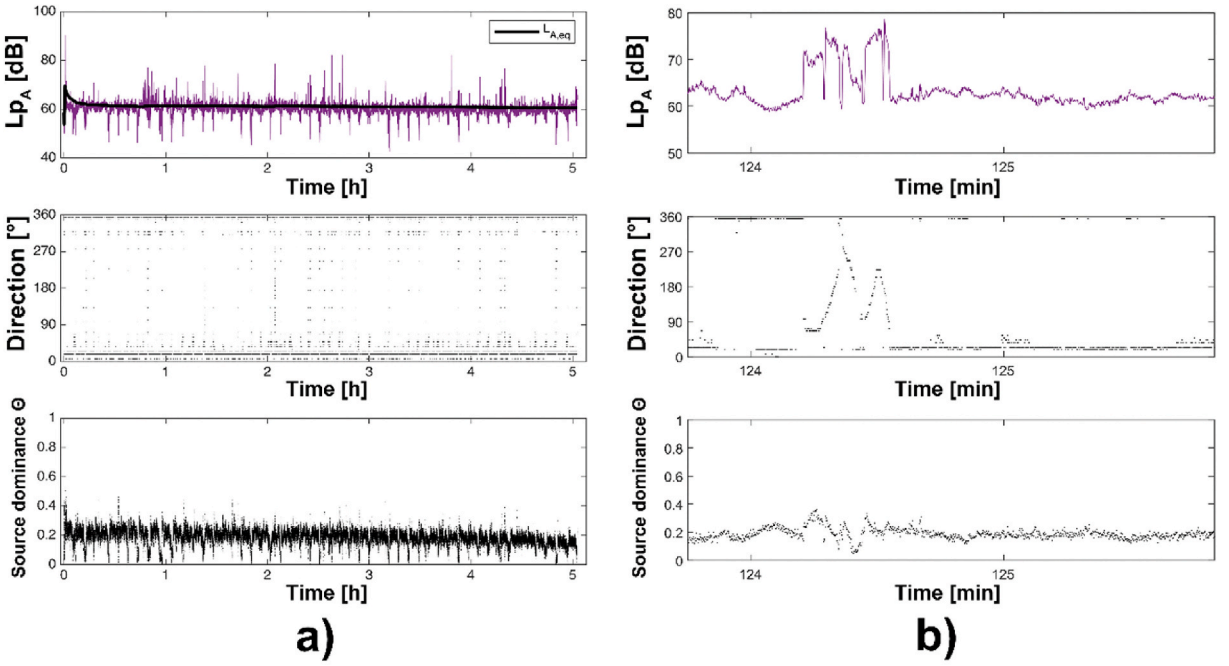

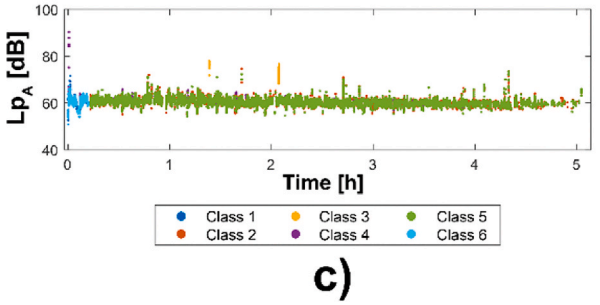

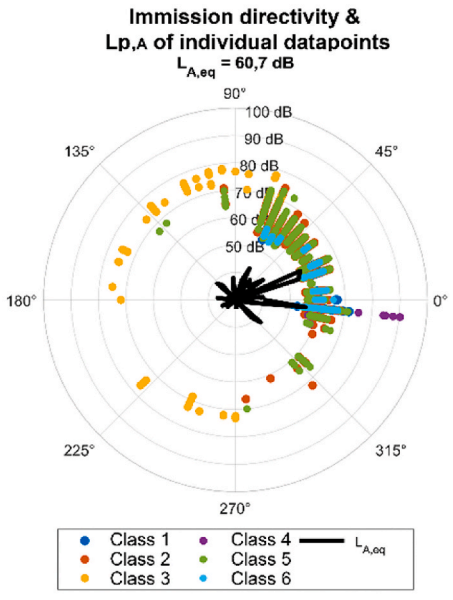

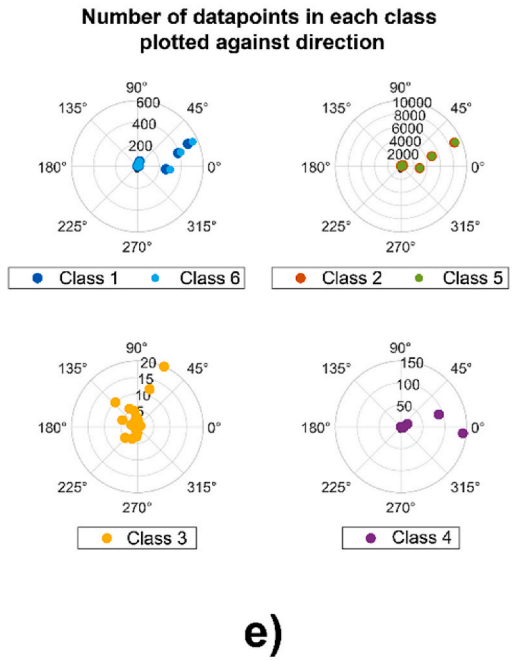

(caption on next page)

Fig. 8. Recorded data of $L_{p,A}$, direction and source dominance Θ from MP2 of: a) The entire measurement, b) Train pass-by. Classified datapoints from MP2 plotted against: c) Time and $L_{p,A}$, d) Direction and $L_{p,A}$ (together with immission directivity), d) direction by their total number in each class.

Summarizing the results presented in Fig. 7 and Table 2, the class 1 and class 7 data points can be attributed to the noise of unloading the load and the movement of the forklift. Class 2 covers the locomotive noise of the passenger train (lower number of data points, higher equivalent level value), while class 5 covers the noise of the railcars (directional scatter and higher number of data points compared to class 2). Classes 3 and 8 represent the noise of a truck and in some cases the diesel locomotive of a freight train, while classes 4 and 6 represent the ventilation of storage facilities/warehouses.

Spatial filtering excluded 86% of the total measured data. From the classified data, we obtained an equivalent level almost 4 dBA lower than the measured one (Table 2), which is the result of eliminating points where the noise level was higher. The reason for this is the spatial filtering based on the stationarity of the direction, since it reaches a large dispersion in the presence of a passing train. We conclude that the detected direction with greater distance from the tracks would be more stationary, consequently bringing the equivalent level obtained with unfiltered datapoints closer to the measured equivalent level.

4.2. Parking lot of Faculty of Mechanical Engineering

The second measurement was performed in the parking lot of the Faculty of Mechanical Engineering of the University of Ljubljana. Noise sources, in addition to passing vehicles and people, were the compressor station and its ventilation system on the first floor of the Laboratory for Pumps, Compressors and Technical Acoustics, and the ventilation duct on the facade of the main building of the Faculty, north of the measurement location. The placement of the array in the parking lot can be seen in Fig. 6.c.

It can be seen that the immission directivity has two prominent lobes to the east, exceeding the A-weighted equivalent level of 55 dBA. The directions 354° and 18° and 24° mark the first floor window and the edge of the wall where the compressor station ventilation is installed. On the polar diagram with a much lower equivalent sound pressure level, other clear directions can be seen: 66° (ventilation duct on the facade of the main faculty building), 36° (intermediate direction between the two vents) and 318° (second slit of the obliquely opened window of the first floor). Although in this measurement there was no doubt about which source contributed the most to the total noise source, additional useful information can be obtained by analyzing the collected data of the whole measurement. The noise level, dominant direction and source dominance Θ as a function of time can be seen in Fig. 8.a.

Short-term drops in the recorded sound pressure level during the measurement clearly indicate that the compressor station was switched off. As a direct consequence, non-stationarity of the determined dominant direction is also observed, which, together with the decrease in the value of the source dominance Θ, indicates the absence of a dominant noise source. Fig. 8.b shows a part of the measurement where the detected dominant direction was stable and the sound pressure level was higher compared to the rest of the measurement. It can be seen that the noise source moved in the range of 90°–270° and lasted less than half a minute, with single interruptions lasting about 1 s.

The next step was to classify the individual sound events. Given the values of source dominance Θ of the entire measurement, as seen in Fig. 8.a, we chose a value of 0.2 as the threshold for spatial filtering. The stationarity angle of the sound incidence direction was the same as in the IZ Šiška measurement (9°). The data points of the recorded sound pressure level, which were divided into six classes, are shown in Fig. 8.c, where three distinct regions can be seen. The data points of classes 1 and 6 occurred at the beginning of the measurement, i.e., in the first 15 min, and the points of classes 2 and 5 occurred essentially during most of the measurement. Class 3 points occurred in two separate occasions, around the 80th and 190th minutes of the measurement.

The polar diagram in Fig. 8.d shows the data points of each class as a function of direction and sound pressure level. It can be seen that the noise from class 3 from the range between 66° and 270°, while the rest of the sound was captured from the range between 0° and 66°, with individual points between 270° and 0°.

Because of the large number of data points, Fig. 8.d is not particularly clear. It was necessary to display the individual classes according to the number of data points they contain. Fig. 8.e shows four polar diagrams. By far the largest number of data points were assigned to classes 2 and 5, i.e., the compressor station ventilation and the duct on the facade of the main faculty building. After listening to the recording, we identified class 4 as a scream that occurred at the beginning of the measurement and several times during the recording of the device to verify that the system was still working. Classes 1 and 6 represent speech coming from the compressor station area. Class 3 represents two specific moments in the measurement when the source was identified as murmurs from casual curious observers near the microphone array.

Summarizing the results of the second measurement in the parking lot of the Faculty of Mechanical Engineering, we can conclude that the compressor station or its ventilation system on the first floor was responsible for most of the noise. We presume that if the

Table 3
Calculated values of $L_{A,eq}$ for each class from spatially filtered data recorded at MP2.

Source	$L_{A,eq}$	Source	$L_{A,eq}$
Class 1	61,1 dBA	Class 6	61,1 dBA
Class 2	60,6 dBA	Class 5	60,7 dBA
Class 3	73,7 dBA	Class 4	70,2 dBA
All classes collectively	**61,1 dBA**	**Entire measurement**	**60,7 dBA**

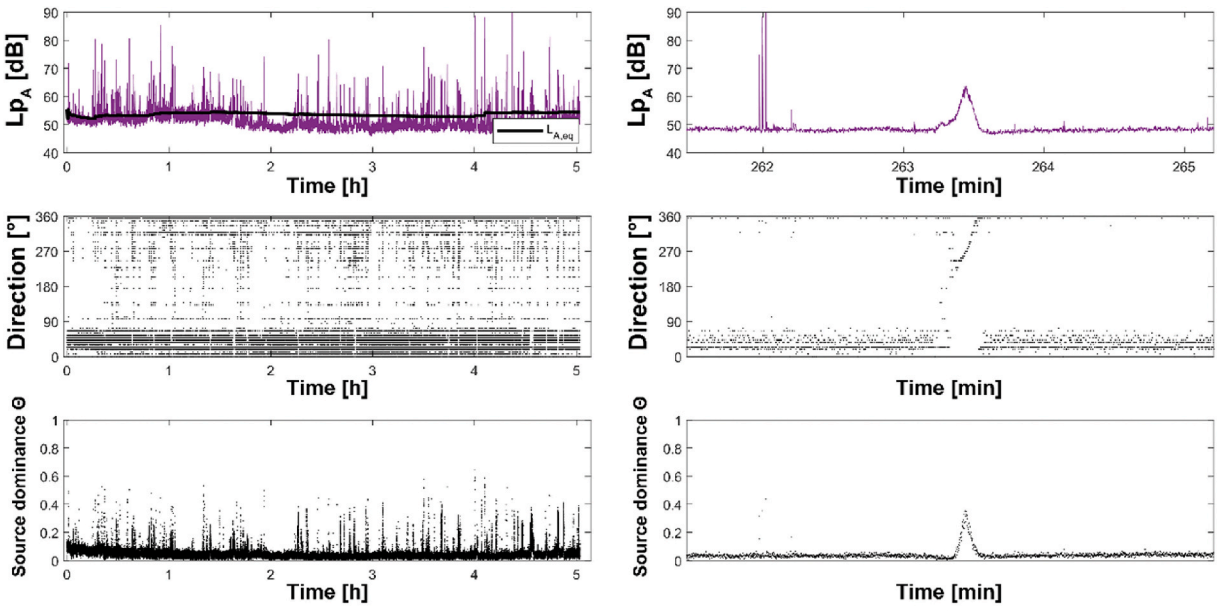

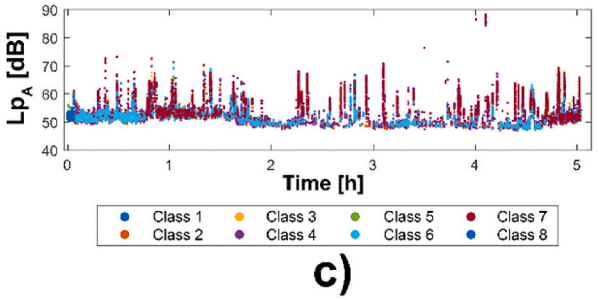

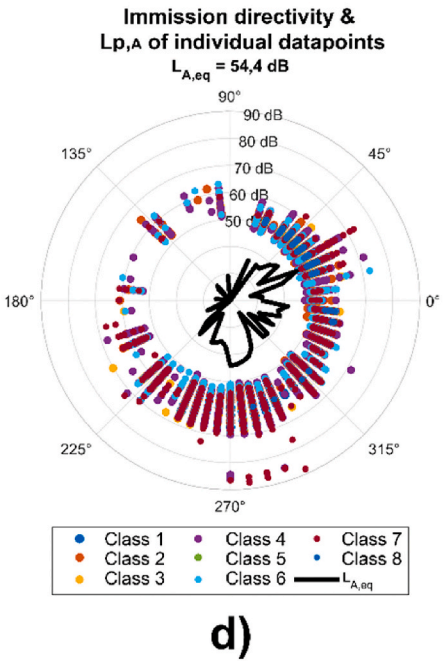

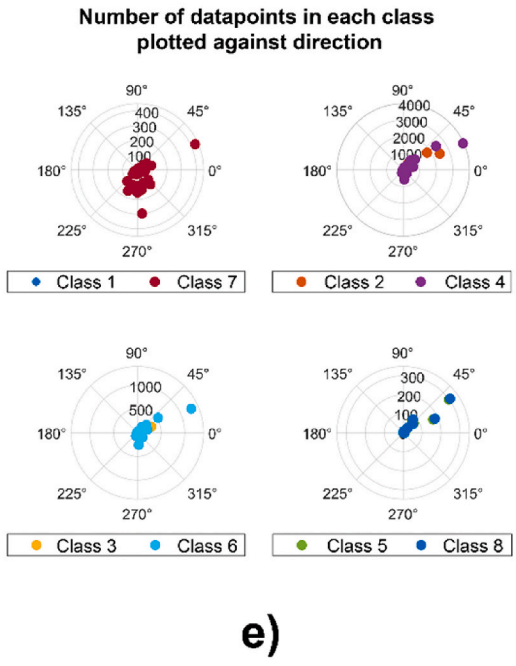

(caption on next page)

Fig. 9. Recorded data of $L_{p,A}$, direction and source dominance Θ from MP3 of: a) The entire measurement, b) Train pass-by. Classified data points from MP3 plotted against: c) Time and $L_{p,A}$, d) Direction and $L_{p,A}$ (together with immission directivity), d) direction by their total number in each class.

window was closed, the results would be different and the direction of the immission would be more balanced towards the ventilation system in the main building of the Faculty. However, this measurement allowed a clear distinction between each source based on spatial filtering and classification based on psychoacoustic characteristics. The determined equivalent level is also comparable to the measured one (Table 3), even though 73% of the measurement was filtered out due to the stationarity of the dominant direction and the source dominance Θ. Classes 2 and 5, which contain the most data points, had the same calculated and measured equivalent sound pressure level as the entire measurement, further confirming that the main noise source at MP2 was the ventilation system and compressor station itself.

4.3. Train station Moste

The third in-situ measurement was conducted near the Moste train station, where noise from passing trains, the Aquafil factory, and the container terminal could be heard. The measurement point was located on the gravel road, near the gardens and tool sheds used by local residents.

Two separate directions can be distinguished by observing the immission directivity plot in Fig. 6.d. Most of the noise was emitted from directions of 24° and 270°, and in general the majority of the noise came from the south and northeast. Short-term increases in SPL can be clearly seen in the data for the entire measurement in Fig. 9.a. This coincides with the scattered detection of the detected dominant direction and the increased source dominance Θ. These values are the consequence of gardening, unloading of containers and other impulse sound sources. Due to the low frequencies, the Θ values were generally the lowest compared to the other two measurements. Although the determined direction was quite non-stationary, we can conclude that most of the noise immission came from the northeast, as shown by the time course of the whole measurement.

The time course of SPL, the dominant direction, and the feature Θ between the 262nd and 265th minutes of the measurement can be seen in Fig. 9.b. With the steady increase of SPL and Θ, the presence of a moving train south from the measurement point can be observed, as well as the impulse sound around the 262nd minute of the measurement. A value of 0.1 was chosen as the threshold for the source dominance feature Θ and an angle of 9° for the stationarity of the detected dominant direction. Fig. 9.c shows the allocation of the data into individual classes as a function of the measurement time. The data points of classes 5 and 8 dominate the section at the beginning of the measurement, while all briefly elevated SPL values are also clearly visible (mainly defined by class 7).

As with MP1 and MP2, the results of MP3 had to be divided into four polar diagrams (see Fig. 9.d). Excluding direction 24°, the train noise came from the range between 225° and 315° and was mostly classified into class 7. Some misclassifications resulted from other impulse noise and container terminal machinery noise. Most of the data were assigned to classes 2 and 4, representing container terminal noise. This was followed by classes 3 and 6, which were identified as low-frequency impulse noise from the tracks and also from the container terminal site after listening to the recording.

When the value of Θ fell below 0.1, the data points with values of SPL were filtered out from the calculation of $L_{A,eq}$, resulting in the equivalent level being 3.4 dBA higher than the value calculated from the whole measurement. If we omit classes 1 and 7, the other values in Table 4 are similar for both approaches. Noise most likely coming from the container terminal and Auqfil industrial complex, containing many low frequencies, was assigned to classes 5 and 8, and the lower dB values can be due to the A-weighting, which reduces their influence. Although the classification is not as clear as we had hoped, the immission directivity clearly indicates the two directions from which most noise arrived to MP3: south and northeast. 81% of the data were excluded due to spatial filtering, on par with cases MP1 and MP2 (86% and 73%, respectively).

5. Discussion

We compared the results of $L_{A,eq}$ of SPL to properly evaluate the prototype system and its assessment of different noise sources. The manual technique of listening and marking individual parts of each of the three measurements was very time consuming and also prone to errors due to the dynamics and noise of the acoustic environment. Comparing the time taken by the two techniques, the system required a maximum of 3 min, while the manual post-processing took more than an hour on average. The comparison of the results can be seen in Table 5.

$L_{A,eq}$ discrepancies between results are inherent because it is impossible to obtain accurate values. In both the manual and auto-

Table 4
Calculated values of $L_{A,eq}$ for each class from spatially filtered data recorded at MP3.

Source	$L_{A,eq}$	Source	$L_{A,eq}$
Class 1	61,9 dBA	Class 7	64,7 dBA
Class 2	52,4 dBA	Class 4	57,0 dBA
Class 3	58,9 dBA	Class 6	55,6 dBA
Class 5	52,3 dBA	Class 8	52,3 dBA
All classes collectively	**57,8 dBA**	**Entire measurement**	**54,4 dBA**

Table 5
$L_{A,eq}$ values extracted from MP1, MP2 and MP3.

MP1 IZ Šiška	$L_{A,eq}$		MP2 Faculty of Mech. Eng.	$L_{A,eq}$		MP3 Train station Moste	$L_{A,eq}$	
	System	Manually		System	Manually		System	Manually
Cargo handling (C1 & 7)	67,0 dBA	66,2 dBA	Speech (C1 & 6)	61,1 dBA	63,5 dBA	Train (C1 & 7)	64,7 dBA	64,9 dBA
Train (C2 & 5)	68,2 dBA	73,4 dBA	Ventilation (C2 & 5)	60,6 dBA	61,3 dBA	Aquafil (C5 & 8)	55,8 dBA	51,6 dBA
Truck (C3 & 8)	62,6 dBA	61,0 dBA	Curious observers (C3)	73,7 dBA	71,4 dBA	Container terminal (C2 & 4)	56,4 dBA	53,0 dBA
Ventilation (C4 & 6)	60,4 dBA	56,7 dBA	Yelling (test) (C4)	70,2 dBA	72,0 dBA	Low frequency impulse noise (C3 & 6)	52,3 dBA	52,9 dBA
Entire measurement	62,6 dBA	66,4 dBA	Entire measurement	61,1 dBA	60,7 dBA	Entire measurement	57,8 dBA	54,4 dBA

mated approaches, individual parts of the measurements are selected, which ultimately leads to data loss. In the manual filtering approach, the accuracy of selection and judgment is most important when listening to the entire 5-h recording, as the selection of representative parts is critical. On the other hand, the results obtained with the automatic method can be affected by quieter sources, (too) large sources, and fast-moving sources near the measurement point. The data is then consequently excluded from the calculation of the $L_{A,eq}$.

In the measurement at MP1 (IZ Šiška), the determined equivalent level values (manually and with the system) of trucks and cargo unloading are comparable. There was a larger deviation for ventilation due to lower sound pressure levels and filtering based on the value of source dominance Θ. The largest deviation was for train noise. Due to the proximity of the tracks to the measurement point and the speed of the train, the system filtered out some higher values of the sound pressure level, resulting in a lower total equivalent level. If we also compare the differences in the total equivalent level (3.8 dBA), we can see that the train noise has a significant influence on the total sound level at MP1.

For MP2, the largest deviations between manually and automatically determined values were for the residual sources (speech, murmuring, shouting). The immission directivity showed that the main source of noise in the parking lot of the Faculty of Mechanical Engineering, UL, was the ventilation of the compressor station. The difference between the marking of the data obtained with the prototype system and the manual marking is the smallest of all three cases, resulting in very similar equivalent levels of the total measurement (0.4 dBA).

As a consequence of the low-frequency noise, the MP3 measurements showed the largest mismatch of $L_{A,eq}$ in the case of the Aquafil factory noise. The stationarity of the detected dominant direction was impaired, especially at low SPL. A similar observation can be made for the container terminal results. We can assume that these two sources are the main reason for the difference in $L_{A,eq}$ between the two approaches, which was 3.4 dBA.

All in all, the results obtained with the presented system were comparable to those obtained manually. By combining the $L_{A,eq}$ values and the immission directivity values, it was possible to identify the main noise sources for all three measurements, thus achieving the main objective of the research. The prototype device and the approach based on the use of spatial domain suggest that conventional measurements may soon be replaced. The evaluation of noise sources will be less costly, time consuming and prone to human error.

6. Conclusions

Noise is an increasing pollutant and represents a major health risk, especially in urban life. For this reason, the approach to identifying noise sources needs to be improved because current approaches are costly, time-consuming, and prone to human error. Due to the dynamic nature and complexity of environmental noise, long measurement times and the need for expensive equipment and trained personnel are required. Simplifying and automating the identification of the main noise sources and excluding residual and background noise enables more effective measurements.

The effectiveness of the proposed system for determining the contribution of each noise source to the total noise level was demonstrated. Long-term measurements provided comparable values for $L_{A,eq}$, and with the implementation of a new concept of immission directivity, correct identification of the main noise sources for all three measurements was possible.

This study shows that the inclusion of spatial domain extends the possibilities of automatic identification of environmental noise sources. Imission directivity and the feature of source dominance Θ proved to be of great value. Therefore, automatic calculation of equivalent sound pressure levels is faster, more reliable, more objective, and less expensive. The combination of localization, spatial filtering, use of psychoacoustic (and other) features, and unsupervised learning proved effective in mimicking the behaviour and experience of trained personnel.

The effect of low-frequency noise on dominant direction detection and consequently on source dominance feature calculation and immission directivity has to be investigated futher. Implemented algorithms need to be adjusted and laboratory experiments conducted. It is expected that an improved localization algorithm will be implemented while maintaining low computational costs so that future versions of the system will still be practical and economical. Further test measurements are planned for will be performed in different acoustic scenarios and together with a detailed the investigation of stationarity of the detected dominant direction of the

sound immission. Nevertheless, the presented device is a step in the right direction to reduce noise pollution more effectively by continuous measurements to identify noise sources.

The results of the presented pilot measurements at different locations in the city of Ljubljana, Slovenia, provided us with exceptional results and a great starting point for further improvements regarding the possibility of automatic identification of environmental noise sources and calculation of their equivalent sound pressure levels.

Declaration of competing interest

The authors declare that they have no known competing financial interests or personal relationships that could have appeared to influence the work reported in this paper.

References

[1] Ramin Rahmani, et al., Body physiological responses of city bus drivers subjected to noise and vibration exposure in working environment, Heliyon 8 (8) (2022), e10329.
[2] Tom Cole-Hunter, et al., Long-term Exposure to Road Traffic Noise and All-Cause and Cause-specific Mortality: a Danish Nurse Cohort Study, Science of The Total Environment, 2022, 153057.
[3] Michael G. Smith, et al., Traffic noise-induced changes in wake-propensity measured with the Odds-Ratio Product (ORP), Sci. Total Environ. 805 (2022), 150191.
[4] Sandra Sanok, et al., Road traffic noise impacts sleep continuity in suburban residents: exposure-response quantification of noise-induced awakenings from vehicle pass-by at night, Sci. Total Environ. 817 (2022), 152594.
[5] Thomas Münzel, Mette Sørensen, Andreas Daiber, Transportation noise pollution and cardiovascular disease, Nat. Rev. Cardiol. (2021) 1–18.
[6] Mette Sørensen, Göran Pershagen, Transportation noise linked to cardiovascular disease independent from air pollution, Eur. Heart J. 40 (2019) 604–606.
[7] Thomas Münzel, et al., Noise and cardiovascular risk: nighttime aircraft noise acutely triggers cardiovascular death, Eur. Heart J. 42 (8) (2021) 844.
[8] Zuzana Kupcikova, et al., Road traffic noise and cardiovascular disease risk factors in UK Biobank, Eur. Heart J. 42 (21) (2021) 2072–2084.
[9] Thomas Münzel, et al., Environmental noise and the cardiovascular system, J. Am. Coll. Cardiol. 71 (6) (2018) 688–697.
[10] Mathias Basner, W. Riggs Daniel, Daniel J. Conklin, Environmental determinants of hypertension and diabetes mellitus: sounding off about the effects of noise, J. Am. Heart Assoc. 9 (6) (2020), e016048.
[11] Danielle Vienneau, et al., Association between Transportation Noise and Cardio-Metabolic Diseases: an Update of the WHO Meta-Analysis, 2019.
[12] Mohammad Javad Zare Sakhvidi, et al., Association between noise exposure and diabetes: a systematic review and meta-analysis, Environ. Res. 166 (2018) 647–657.
[13] Charlotta Eriksson, Göran Pershagen, Mats Nilsson, Biological Mechanisms Related to Cardiovascular and Metabolic Effects by Environmental Noise. No. WHO/EURO: 2018-3009-42767-59666, World Health Organization. Regional Office for Europe, 2018.
[14] Laurie Thiesse, et al., Adverse impact of nocturnal transportation noise on glucose regulation in healthy young adults: effect of different noise scenarios, Environ. Int. 121 (2018) 1011–1023.
[15] Zorana J. Andersen, et al., Long-term exposure to road traffic noise and air pollution, and incident atrial fibrillation in the Danish Nurse Cohort, Environ. Health Perspect. 129 (8) (2021), 087002.
[16] Omar Hahad, et al., The cardiovascular effects of noise, Deutsches Ärzteblatt Int. 116 (14) (2019) 245.
[17] Shuo Liu, et al., Long-term exposure to ambient air pollution and road traffic noise and asthma incidence in adults: the Danish Nurse cohort, Environ. Int. 152 (2021), 106464.
[18] Wallas, Alva Enoksson, et al., Noise exposure and childhood asthma up to adolescence, Environ. Res. 185 (2020), 109404.
[19] Paraskevi Begou, Pavlos Kassomenos, Exposure to the road traffic noise in an urban complex in Greece: the quantification of healthy life years lost due to noise-induced annoyance and noise-induced sleep disturbances, Environ. Sci. Pollut. Control Ser. 28 (10) (2021) 12932–12943.
[20] Clémence Baudin, et al., The role of aircraft noise annoyance and noise sensitivity in the association between aircraft noise levels and medication use: results of a pooled-analysis from seven European countries, BMC Publ. Health 21 (1) (2021) 1–15.
[21] Janice Hegewald, et al., Traffic noise and mental health: a systematic review and meta-analysis, Int. J. Environ. Res. Publ. Health 17 (17) (2020) 6175.
[22] Yutong Cai, et al., Impact of road traffic noise on obesity measures: observational study of three European cohorts, Environ. Res. 191 (2020), 110013.
[23] Rhiannon Thompson, et al., Noise pollution and human cognition: an updated systematic review and meta-analysis of recent evidence, Environ. Int. 158 (2022), 106905.
[24] Yifan Zhang, et al., Environmental noise degrades hippocampus-related learning and memory, Proc. Natl. Acad. Sci. USA 118 (1) (2021).
[25] Eulalia Peris, Environmental noise in Europe: 2020, Eur. Environ. Agency 1 (2020) 104.
[26] Bocanegra, Johan Augusto, et al., A novel approach to port noise characterization using an acoustic camera, Sci. Total Environ. 808 (2022), 151903.
[27] Luka Čurović, et al., Impact of COVID-19 on environmental noise emitted from the port, Sci. Total Environ. 756 (2021), 144147.
[28] Luca Fredianelli, et al., Source characterization guidelines for noise mapping of port areas, Heliyon 8 (3) (2022), e09021.
[29] Pablo Kogan, et al., A Green Soundscape Index (GSI): the potential of assessing the perceived balance between natural sound and traffic noise, Sci. Total Environ. 642 (2018) 463–472.
[30] A. Ruiz-Padillo, D.P. Ruiz, A.J. Torija, Á. Ramos-Ridao, Selection of suitable alternatives to reduce the environmental impact of road traffic noise using a fuzzy multi-criteria decision model, Environ. Impact Assess. Rev. 61 (2016) 8–18.
[31] D. Petri, G. Licitra, M.A. Vigotti, L. Fredianelli, Effects of exposure to road, railway, airport and recreational noise on blood pressure and hypertension, Int. J. Environ. Res. Publ. Health 18 (17) (2021) 9145.
[32] M. Nastasi, L. Fredianelli, M. Bernardini, L. Teti, F. Fidecaro, G. Licitra, Parameters affecting noise emitted by ships moving in port areas, Sustainability 12 (20) (2020) 8742.
[33] Paulo Henrique Trombetta Zannin, et al., Evaluation of environmental noise generated by household waste collection trucks, J. Environ. Assess. Pol. Manag. 20 (4) (2018), 1850010.
[34] Consolatina Liguori, et al., Accurate estimation of the environmental noise through sampling approach: selection of the measurement time, IEEE Trans. Instrum. Meas. 67 (5) (2018) 1006–1013.
[35] B. Berglund, T. Lindvall, Community Noise, Center for Sensory Research, Švedska, 1995.
[36] Birgitta Berglund, Peter Hassmen, RF Soames Job, Sources and effects of low-frequency noise, J. Acoust. Soc. Am. 99 (5) (1996) 2985–3002.
[37] T.D. Rossing, Springer Handbook of Acoustics, Stanford University, Center for Computer Research in Music and Acoustics, ZDA, 2007.
[38] Arnaud Can, et al., Traffic noise spectrum analysis: dynamic modeling vs. experimental observations, Appl. Acoust. 71 (8) (2010) 764–770.
[39] Antonio J. Torija, Ian H. Flindell, Differences in subjective loudness and annoyance depending on the road traffic noise spectrum, J. Acoust. Soc. Am. 135 (1) (2014) 1–4.
[40] Oleksandr Zaporozhets, et al., Indoor noise A-level assessment related to the environmental noise spectrum on the building facade, Appl. Acoust. 185 (2022), 108380.
[41] P. Maijala, Z. Shuyang, T. Heittola, T. Virtanen, Environmental noise monitoring using source classification in sensors, Appl. Acoust. 129 (2018) 258–267.
[42] J. Prezelj, Directivity Measurements of Environmental Noise Immission, Euronoise, Crete, 2018, pp. 711–717.

[43] Jon-Paul Faulkner, Enda Murphy, Estimating the harmful effects of environmental transport noise: an EU study, Sci. Total Environ. 811 (2022), 152313.
[44] Juan Miguel Barrigón Morillas, David Montes González, Guillermo Rey Gozalo, A review of the measurement procedure of the ISO 1996 standard. Relationship with the European Noise Directive, Sci. Total Environ. 565 (2016) 595–606.
[45] W. Wei, T. Van Renterghem, B. De Coensel, D. Botteldooren, Dynamic noise mapping: a map based interpolation between noise measurements with high temporal resolution, Appl. Acoust. 101 (2016) 127–140.
[46] J. Prezelj, J. Murovec, Traffic noise modelling and measurement: inter-laboratory comparison, Appl. Acoust. 127 (2017) 160–168.
[47] Pierre Aumond, et al., Global sensitivity analysis for road traffic noise modelling, Appl. Acoust. 176 (2021), 107899.
[48] Vassiliki Delitheou, Efthimios Bakogiannis, Charalampos Kyriakidis, Urban planning: integrating smart applications to promote community engagement, Heliyon 5 (5) (2019), e01672.
[49] Arnaud Can, et al., CENSE Project: General Overview, in: Euronoise. Presented at the Euronoise, Madeira, Portugal-e-congress, 2021.
[50] Miroslav Němec, et al., Selected approaches to the assessment of environmental noise from railways in urban areas, Int. J. Environ. Res. Publ. Health 18 (13) (2021) 7086.
[51] Anna Eszter Engedy, Josef Lechleitner, Ardeshir Mahdavi, Sound propagation in urban canyons: a case study of simulation reliability, J. Build. Perform. Simul. 12 (4) (2019) 363–377.
[52] G. Zambon, R. Benocci, G. Brambilla, Cluster categorization of urban roads to optimize their noise monitoring, Environ. Monit. Assess. 188 (1) (2016) 1–11.
[53] Muxiao Li, et al., Analysis of source contribution to pass-by noise for a moving high-speed train based on microphone array measurement, Measurement 174 (2021), 109058.
[54] Paolo Chiariotti, Milena Martarelli, Paolo Castellini, Acoustic beamforming for noise source localization–Reviews, methodology and applications, Mech. Syst. Signal Process. 120 (2019) 422–448.
[55] Roberto Merino-Martinez, et al., Sound Quality Metrics Applied to Aircraft Components under Operational Conditions Using a Microphone Array, in: 25th AIAA/CEAS Aeroacoustics Conference, 2019.
[56] Hongyan Xing, Xu Yang, Sound source localization fusion algorithm and performance analysis of a three-plane five-element microphone array, Appl. Sci. 9 (12) (2019) 2417.
[57] Matthew Aldeman, Ganesh Raman, Effects of array scaling and advanced beamforming algorithms on the angular resolution of microphone array systems, Appl. Acoust. 132 (2018) 58–81.
[58] Wei Ma, et al., Beamforming of phased microphone array for rotating sound source localization, J. Sound Vib. 467 (2020), 115064.
[59] Yonggang Hu, Prasanga N. Samarasinghe, Thushara D. Abhayapala, Sound Source Localization Using Relative Harmonic Coefficients in Modal Domain, in: 2019 IEEE Workshop on Applications of Signal Processing to Audio and Acoustics (WASPAA), IEEE, 2019.
[60] Naoto Iijima, Shoichi Koyama, Hiroshi Saruwatari, Binaural rendering from microphone array signals of arbitrary geometry, J. Acoust. Soc. Am. 150 (4) (2021) 2479–2491.
[61] In-Jee Jung, Jeong-Guon Ih, Combined microphone array for precise localization of sound source using the acoustic intensimetry, Mech. Syst. Signal Process. 160 (2021), 107820.
[62] Lei Li, et al., Acoustic enhanced camera tracking system based on small-aperture MEMS microphone array, IEEE Access 8 (2020) 215827–215839.
[63] Lei Li, et al., SuperSoundcompass: a high-accuracy acoustic localization sensor using a small-aperture microphone array, Meas. Sci. Technol. 32 (10) (2021), 105106.
[64] Weijie Qian, et al., Design of a three degrees-of-freedom biomimetic microphone array based on a coupled circuit, Meas. Sci. Technol. 30 (6) (2019), 065101.
[65] Imrich Andráš, et al., Beamforming with Small Diameter Microphone Array, in: 2018 28th International Conference Radioelektronika, IEEE, 2018.
[66] J. Tiete, F. Dominguez, B. da Silva, L. Segers, K. Steenhaut, Abdellah Touhafi, SoundCompass: a distributed MEMS microphone array-based sensor for sound source localization, Sensors 14 (2014) 1918–1949.
[67] Elisabet Tiana-Roig, Finn Jacobsen, Efrén Fernández Grande, Beamforming with a circular microphone array for localization of environmental noise sources, J. Acoust. Soc. Am. 128 (6) (2010) 3535–3542.
[68] Xin Zhang, et al., Design of small MEMS microphone array systems for direction finding of outdoors moving vehicles, Sensors 14 (3) (2014) 4384–4398.
[69] Gabriela Dantas Rocha, et al., Direction of Arrival Estimation of Partial Sound Sources of Vehicles with a Two-Microphone Array, 2021, p. 18.
[70] Mark L. Moran, Roy J. Greenfield, D. Keith Wilson, Acoustic array tracking performance under moderately complex environmental conditions, Appl. Acoust. 68 (10) (2007) 1241–1262.
[71] Meritxell Genescà, et al., Measurement of aircraft noise in a high background noise environment using a microphone array, Transport. Res. Transport Environ. 18 (2013) 70–77.
[72] Kanthasamy Chelliah, et al., Demonstration of the possibilities of using a phased microphone array as the next-generation airport noise monitoring system, Transport. Res. Rec. 2600 (1) (2016) 20–26.
[73] Miloš Bjelić, et al., Microphone array geometry optimization for traffic noise analysis, J. Acoust. Soc. Am. 141 (2017) 5.
[74] Xingshui Zu, et al., Design of an acoustic target intrusion detection system based on small-aperture microphone array, Sensors 17 (3) (2017) 514.
[75] Wei Ma, Xun Liu, Phased microphone array for sound source localization with deep learning, Aero. Syst. 2 (2) (2019) 71–81.
[76] L. Fredianelli, M. Bernardini, F. Tonetti, F. Artuso, F. Fidecaro, G. Licitra, Acoustic Source Localization in Ports with Different Beamforming Algorithms, in: Proceedings of 51st INTER-NOISE Congress, Glasgow, 2022, pp. 21–24.
[77] Bahaa Al-Sheikh, et al., Sound Source Direction Estimation in Horizontal Plane Using Microphone Array, in: 2013 IEEE Jordan Conference on Applied Electrical Engineering and Computing Technologies (AEECT), IEEE, 2013, https://doi.org/10.1109/AEECT.2013.6716479.
[78] Jure Murovec, et al., Microphone array based automated environmental noise measurement system, Appl. Acoust. 141 (2018) 106–114, https://doi.org/10.1016/j.apacoust.2018.07.004.
[79] J. Prezelj, L. Curovic, T. Novakovic, J. Murovec, Estimation of Noise Immission Directivity Using Small Microphone Array, Universitätsbibliothek der RWTH Aachen, 2019.
[80] Jure Murovec, et al., Environmental Noise Event Classification Based on Self-Organizing Map Using Psychoacoustic Features and Spatial Filtering, Universitätsbibliothek der RWTH Aachen, 2019.
[81] Jurij Prezelj, et al., A novel approach to localization of environmental noise sources: sub-windowing for time domain beamforming, Appl. Acoust. 195 (2022), 108836.
[82] Wen Zhao, Bo Yin, Environmental Sound Classification Based on Adding Noise, in: 2021 IEEE 2nd International Conference on Information Technology, Big Data and Artificial Intelligence (ICIBA), vol. 2, IEEE, 2021.
[83] Fatih Demir, Daban Abdulsalam Abdullah, Abdulkadir Sengur, A new deep CNN model for environmental sound classification, IEEE Access 8 (2020).
[84] Jiuwen Cao, et al., Urban noise recognition with convolutional neural network, Multimed. Tool. Appl. 78 (20) (2019) 29021–29041.
[85] Zohaib Mushtaq, Shun-Feng Su, Environmental sound classification using a regularized deep convolutional neural network with data augmentation, Appl. Acoust. 167 (2020), 107389.
[86] J. Salamon, J.P. Bello, Feature Learning with Deep Scattering for Urban Sound Analysis, in: Proc. 2015 23rd Eur. Signal Process. Conf., 2015, pp. 724–728.
[87] K.J. Piczak, Environmental Sound Classification with Convolutional Neural Networks, in: 2015 IEEE 25th International Workshop on Machine Learning for Signal Processing (MLSP), IEEE, 2015, September, pp. 1–6.
[88] J. Salamon, J.P. Bello, Deep convolutional neural networks and data augmentation for environmental sound classification, IEEE Signal Process. Lett. 24 (3) (2017) 279–283.
[89] S. Sigtia, A.M. Stark, S. Krstulović, M.D. Plumbley, Automatic environmental sound recognition: performance versus computational cost, IEEE/ACM Trans. Audio, Speech, Lang. Process. 24 (11) (2016) 2096–2107.
[90] Luis A. Sanchez-Perez, et al., Airport take-off noise assessment aimed at identify responsible aircraft classes, Sci. Total Environ. 542 (2016) 562–577.

[91] S. Chandrakala, S.L. Jayalakshmi, Environmental audio scene and sound event recognition for autonomous surveillance: a survey and comparative studies, ACM Comput. Surv. 52 (3) (2019) 1–34.
[92] R. Haghmaram, A. Aroudi, M.H. Ghezel, H. Veisi, Automatic Noise Recognition Based on Neural Network Using LPC and MFCC Feature Parameters, in: 2012 Federated Conference on Computer Science and Information Systems (FedCSIS), IEEE, 2012, September, pp. 69–73.
[93] M. Pavlović, G. Zajić, M. Zajeganović, D. Ristić, I. Reljin, M. Mijić, Classification of Room Impulse Responses Using Kohonen Neural Network, in: 2018 14th Symposium on Neural Networks and Applications (NEUREL), IEEE, 2018, November, pp. 1–5.
[94] H.-U. Bauer, Thomas Villmann, Growing a hypercubical output space in a self-organizing feature map, IEEE Trans. Neural Network. 8 (2) (1997) 218–226.
[95] Fatemeh Saki, Nasser Kehtarnavaz, Real-time unsupervised classification of environmental noise signals, IEEE/ACM Trans. Audio, Speech, Lang. Process. 25 (8) (2017) 1657–1667.
[96] Abhilasha Sukhwal, Mahendra Kumar, Comparative Study of Different Classifiers Based Speaker Recognition System Using Modified MFCC for Noisy Environment, in: 2015 International Conference on Green Computing and Internet of Things (ICGCIoT), IEEE, 2015.
[97] Sitao Wu, Tommy WS. Chow, Induction machine fault detection using SOM-based RBF neural networks, IEEE Trans. Ind. Electron. 51 (1) (2004) 183–194.
[98] Bo-Suk Yang, Tao Han, J.L. An, ART–KOHONEN neural network for fault diagnosis of rotating machinery, Mech. Syst. Signal Process. 18 (3) (2004) 645–657.
[99] Ali Uysal, Raif Bayir, Real-time condition monitoring and fault diagnosis in switched reluctance motors with Kohonen neural network, J. Zhejiang Univ. - Sci. C 14 (12) (2013) 941–952.
[100] Gang Cheng, et al., Gear fault identification based on Hilbert–Huang transform and SOM neural network, Measurement 46 (3) (2013) 1137–1146.
[101] Emin Germen, Murat Başaran, Mehmet Fidan, Sound based induction motor fault diagnosis using Kohonen self-organizing map, Mech. Syst. Signal Process. 46 (1) (2014) 45–58.
[102] Nikolina Rako, Ivica Vilibić, Hrvoje Mihanović, Mapping underwater sound noise and assessing its sources by using a self-organizing maps method, J. Acoust. Soc. Am. 133 (3) (2013) 1368–1376.
[103] Andrzej Zak, Kohonen Networks as Hydroacoustic Signatures Classifier, in: Proceedings of the 9th WSEAS International Conference on Neural Networks, World Scientific and Engineering Academy and Society (WSEAS), 2008.
[104] G. Cammarata, Salvatore Cavalieri, A. Fichera, A neural network architecture for noise prediction, Neural Network. 8 (6) (1995) 963–973.
[105] N. Genaro, et al., A neural network based model for urban noise prediction, J. Acoust. Soc. Am. 128 (4) (2010) 1738–1746.
[106] Kranti Kumar, Manoranjan Parida, Katiyar Vinod Kumar, Road traffic noise prediction with neural networks-a review, An Int. J. Optim. Control Theor. Appl. (IJOCTA) 2 (1) (2011) 29–37.
[107] G. Cammarata, et al., Self-organizing Map to Filter Acoustic Mapping Survey in Noise Pollution Analysis, in: Proceedings of 1993 International Conference on Neural Networks (IJCNN-93-Nagoya, Japan), vol. 2, IEEE, 1993.
[108] Damiano Oldoni, et al., Context-dependent Environmental Sound Monitoring Using SOM Coupled with LEGION, in: The 2010 International Joint Conference on Neural Networks (IJCNN), IEEE, 2010.
[109] Xavier Valero, et al., Support Vector Machines and Self-Organizing Maps for the Recognition of Sound Events in Urban Soundscapes, in: 41st International Congress and Exposition on Noise Control Engineering (Inter-noise-2012), Institute of Noise Control Engineering, 2012.
[110] Paola Ricciardi, et al., Sound quality indicators for urban places in Paris cross-validated by Milan data, J. Acoust. Soc. Am. 138 (4) (2015) 2337–2348.
[111] Arnaud Can, Benoit Gauvreau, Describing and classifying urban sound environments with a relevant set of physical indicators, J. Acoust. Soc. Am. 137 (1) (2015) 208–218.
[112] Damiano Oldoni, et al., The acoustic summary as a tool for representing urban sound environments, Landsc. Urban Plann. 144 (2015) 34–48.
[113] Eberhard Zwicker, Hugo Fastl, Psychoacoustics: Facts and Models, vol. 22, Springer Science & Business Media, 2013.
[114] Ming Yang, Yu Lei, Herweg Andreas, Automated Environmental Sound Recognition for Soundscape Measurement and Assessment, in: Proceedings of the INTER-NOISE, 2019.
[115] Duque-Montoya, Diana Carolina, Claudia Isaza, Automatic Ecosystem Identification Using Psychoacoustical Features, in: Proceedings of the International Conference on Pattern Recognition and Artificial Intelligence, 2018.
[116] Jesus Lopez-Ballester, et al., Enabling real-time computation of psycho-acoustic parameters in acoustic sensors using convolutional neural networks, IEEE Sensor. J. 20 (19) (2020) 11429–11438.
[117] Haoze Chen, Zhijie Zhang, Hybrid neural network based on novel audio feature for vehicle type identification, Sci. Rep. 11 (1) (2021) 1–10.
[118] Margret Sibylle Engel, et al., A review of the use of psychoacoustic indicators on soundscape studies, Curr. Pollut. Rep. 7 (3) (2021) 359–378.
[119] Ulrich Moehler, Christine Huth, Manfred Liepert, Case studies on the application of psychoacoustic methods for traffic noise, Forum Acust. (2020) 2421–2424.
[120] Klaus Genuit, Binaural measurement and psychoacoustic analysis—an advantage for the environmental noise research, J. Acoust. Soc. Am. 145 (3) (2019) 1752–1753.
[121] Alice Hoffmann, Wolfgang Kropp, Auralization of simulated tyre noise: psychoacoustic validation of a combined model, Appl. Acoust. 145 (2019).
[122] Frits Van den Berg, Wind Farm Noise Management Based on Determinants of Annoyance, 2022.
[123] Steven Cooper, Wind Turbine Noise: Psychoacoustics to the Rescue, in: Forum Acusticum, 2020.
[124] Waldemar Paszkowski, Andrzej Loska, The use of data mining methods for the psychoacoustic assessment of noise in urban environment, Int. Multidiscipl. Sci. GeoConference: SGEM: Surv. Geol. Min. Ecol. Manag. 17 (2017) 1059–1066.
[125] Jure Murovec, et al., Psychoacoustic approach for cavitation detection in centrifugal pumps, Appl. Acoust. 165 (2020), 107323.
[126] Prezelj, Jurij, and Wolfgang Fellner. "System for Automatic Noise Source Identification and Classification." Patent, G01H 11.00: 24518.
[127] Primož Lipar, et al., Automatic recognition of machinery noise in the working environment, Strojniški vestnik-J. Mech. Eng. 61 (2015) 12.
[128] Slovenian Environment Agency. http://gis.arso.gov.si/atlasokolja/profile.aspx?id=Atlas_Okolja_AXL@Arso.